JOURNAL OF PROPULSION AND POWER
Vol. 21, No. 1, January–February 2005

Suppression of Premature Ignition in the Premixed Inlet Flow of a Shcramjet

Thomas E. Schwartzentruber* and Jean P. Sislian†
University of Toronto Institute for Aerospace Studies, Downsview, Ontario M3H 5T6, Canada
and
Bernard Parent‡
Seoul National University, Seoul 151-744, Republic of Korea

The problem of premature ignition in a shock-induced combustion ramjet (shcramjet) inlet is addressed. Previous studies of fuel injection in the inlet have developed fuel injectors and inlet configurations that maximize the mixing efficiency in a shcramjet inlet while maintaining inlet losses at a minimum. A chemically reacting study of the recommended shcramjet inlet configurations finds premature ignition to occur primarily in the boundary layer in the last 15% of the inlet, spreading into the core flow before the inlet exit. Both gaseous nitrogen and additional hydrogen are then injected into the inlet flowfield in an attempt to suppress the flame. Premature ignition is suppressed most feasibly by the injection of additional hydrogen through a backward-facing step (slot injector) located just before the second inlet shock, such that the global equivalence ratio of the premixed flow exiting the inlet is one. The performance of the original inlet remains unaltered, and the frictional force on the inlet wall is reduced by 10% due to the hydrogen slot injection. All turbulent, chemically reacting, three-dimensional, mixing flowfields are solved using the WARP code, which solves the Favre-averaged Navier–Stokes equations closed by the Wilcox $k\omega$ turbulence model and the Wilcox dilatational dissipation correction. Chemical kinetics are modeled by a 9-species, 20-reaction model by Jachimowski.

Nomenclature

c	=	species mass fraction
$\mathcal{F}_{\text{skin friction}}$	=	force vector due to skin friction
k	=	turbulence kinetic energy
M_c	=	convective Mach number, $(q_1 - q_2)/(a_1 + a_2)$
$\dot{m}_{\text{air, engine}}$	=	mass flow rate of air in the engine
P	=	pressure
q	=	magnitude of the velocity vector
T	=	temperature
x, y, z	=	Cartesian coordinates
y^+	=	nondimensional wall distance, $(y/\mu)\sqrt{(\rho\tau_w)}$
η_m	=	mixing efficiency
μ	=	viscosity
τ_w	=	wall shear stress
ϕ	=	equivalence ratio
ϕ_g	=	global equivalence ratio
ω	=	dissipation rate per unit of turbulence kinetic energy

Subscript

b	=	station of interest

Superscripts

R	=	reacting
S	=	stoichiometric

Presented as Paper 2003-5187 at the 39th Joint Propulsion Conference and Exhibit, Huntsville, AL, 21–24 July 2003; received 9 January 2004; revision received 6 July 2004; accepted for publication 8 July 2004.

*Graduate Student, Department of Aerospace Engineering; tom.schwartzentruber@utoronto.ca.
†Professor, Department of Aerospace Engineering; sislian@caius.utias.utoronto.ca. Associate Fellow AIAA.
‡Research Associate, Department of Aerospace Engineering; bernard@snu.ac.kr.

Introduction

AN alternate hypersonic airbreathing propulsion concept to the scramjet is the shock-induced combustion ramjet (shcramjet[1,2]), which is shown in Fig. 1. Whereas scramjet concepts rely on the diffusive burning of injected fuel, the shcramjet concept aims to avoid a long combustion chamber by injecting the fuel in the inlet of the vehicle and burning the fuel/air mixture through a shock wave. This reduces the weight of the engine and takes advantage of the typically long inlets found at hypervelocities. To establish the shcramjet as a viable concept, shcramjet research must seriously address the tasks 1) of achieving adequate fuel/air mixing before the shock-induced combustion and 2) of preventing premature ignition of the premixed combustible flow in the inlet.

The problem of efficient mixing in supersonic flow has been studied in detail with respect to scramjet combustors. Reference 3 provides a recent review of this research. In regard to injecting fuel in a scramjet inlet (before the combustor), Livingston et al.[4] and Owens et al.[5] carried out an experiment where liquid JP-10 fuel was preinjected through pylons situated in a scramjet isolator. In addition, Guskov et al. performed a similar numerical investigation, where pylons were used to inject gaseous hydrocarbon fuel in a scramjet inlet.[6] Results from these studies show significant improvement in the mixing and burning performance of the scramjets, due to preinjection of the fuel before the combustor. Also, these studies demonstrate how pylon injection keeps fuel out of the boundary layer and, thus, prevents flashback.

The task of achieving adequate fuel/air mixing in an external-compression shcramjet inlet has been attempted in Ref. 7. A new injector has been proposed specifically for fuel injection in a shcramjet inlet. Named the cantilevered ramp injector,[8] the injector is based on the standard ramp injector of Marble et al.,[9] with the noted difference of an air buffer between the fuel and the wall at the point of injection to prevent fuel from being injected in the vicinity of the hot incoming boundary layer (Fig. 2). The strong axial vortices generated by the cantilevered ramp injector increase the fuel penetration while maintaining the injection angle low enough to recover most of the thrust due to the fuel momentum. Studies have been performed to determine the effect of the fuel inflow conditions[10] and the injector geometry[11] on the mixing performance of the cantilevered ramp injector over a flat plate. An optimal cantilevered ramp injector

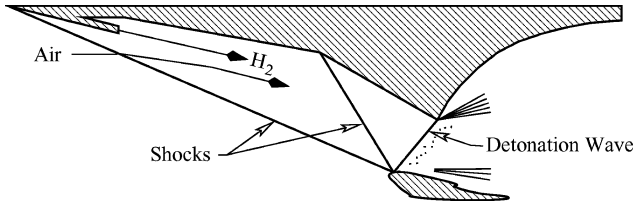

Fig. 1 External compression shcramjet schematic.

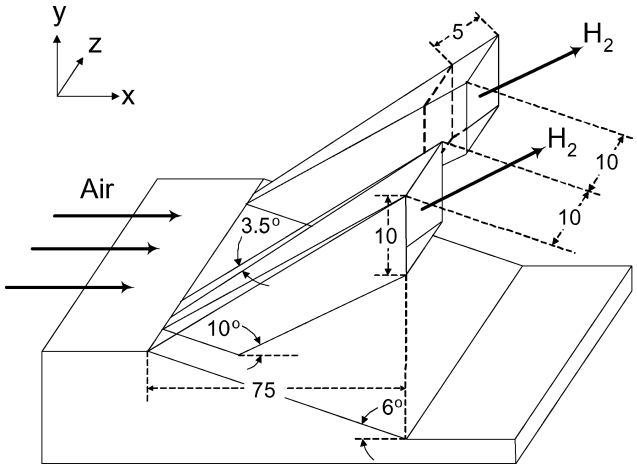

Fig. 2 Optimized cantilevered injector geometry (dimensions in millimeters) taken from a previous study.[7]

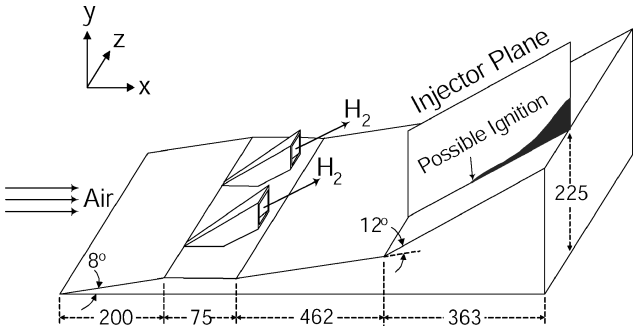

Fig. 3 Baseline dual-spike shcramjet inlet (dimensions in millimeters) taken from a previous study.[7]

configuration (Fig. 2) was selected and used to study the mixing performance in a nonreacting model of an external-compression shcramjet inlet flying at Mach 11 and 34.5-km altitude.[7] The optimized array of cantilevered ramp injectors was mounted on a dual spike (equal shock strength) inlet resulting in the configuration shown in Fig. 3. The main focus of the study was to modify strategically the inlet and injector geometry in an attempt to improve the overall performance of the inlet with respect to the mixing efficiency, the inlet losses, and the risk of premature ignition. Although successful in obtaining a mixing efficiency of 30%, all inlets exposed a near stoichiometric fuel/air mixture to ignition temperatures either in the core flow or in the boundary layer.[7] Thus, premature ignition (as shown in Fig. 3) remained very likely.

The primary objectives of the present paper are to 1) determine the location of premature ignition and the extent of combustion in the previously optimized shcramjet inlet,[7] 2) attempt to suppress premature ignition by injecting nitrogen, or perhaps additional hydrogen gas at strategic locations, and 3) minimize the amount of coolant gas necessary to prevent premature ignition, while not deteriorating the performance of the inlet. Because relevant experimental data on fuel burning in hypersonic boundary layers are absent in the open scientific literature, the results obtained in, and the conclusions drawn from, the present study are solely based on the numerical modeling and simulation described in the next section.

Numerical Model and Error Assessment

The numerical simulation was performed using the WARP code,[10,12] in which the multispecies Favre-averaged Navier–Stokes (FANS) equations closed by the Wilcox $k\omega$ turbulence model[13] are discretized by the Yee–Roe flux-limited method (see Ref. 14). To account for the compressibility effects occurring at high turbulent Mach numbers,[10] the Wilcox dilatational–dissipation correction[15] is used. The chemical source term is calculated using a 20-reaction, 9-species chemical model from Jachimowski.[16] Specific heat and specific entropy are determined from polynomials in function of temperature from McBride and Reno.[17] Convergence to steady state is achieved by block-implicit approximate factorization, including the analytical Jacobians derived from the chemical model. Convergence is then accelerated by using the marching window acceleration technique.[12] The use of the marching window decreases the computational work by 10–20 times and the memory required by 5 times for the inlet cases shown herein and permits the use of significantly finer meshes, hence, resulting in a decreased numerical error.

The computational domain begins at the tip of the inlet and stretches in the x direction just downstream of the intersection of the two inlet shocks. In the y direction, the domain is bounded from below by the inlet wall and is treated as supersonic outflow in the freestream flow above the inlet shocks. In the z direction, the domain begins in the center of a cantilevered injector and ends at half the distance to the next injector (dimensions shown in Fig. 2). Because of the symmetry of the injector array, second-order symmetry boundary conditions are imposed on the sides of the computational domain. For the flowfields analyzed herein, all walls are assumed to be maintained at 500 K and wall spacing is set to 30 μm for the 8-deg wedge and injector surfaces and lowered to 10 μm for the remainder of the inlet. This results in a y^+ distribution that remains between 1 and 4 on all surfaces. In general, the value of y^+ on the inlet wall is seen to increase while moving downstream and reaches its maximum value of 4 at the domain exit. The hydrogen and/or nitrogen develop an incoming boundary layer before injection via a short 5-mm enclosed runway (shown later), which also reduces the solution's sensitivity to the freestream value of ω. As suggested by Wilcox,[18] the inflow value of ω is set to 10 times the inflow velocity and the freestream value of k is initially set to zero. The turbulent Prandtl and Schmidt numbers are set to 0.9 and 1.0, respectively. Finally, the entropy correction term is not used in the Roe scheme because it has no effect on the current inlet flowfield other than to increase the artificial dissipation and, thus, increase the grid induced error (see Ref. 7).

These numerical strategies are based on a thorough investigation[10] of the numerical parameters used by WARP and their effects on supersonic mixing flowfields. The turbulence models and the hydrogen/air chemical kinetics used in the flowfield modeling have been validated in Refs. 19 and 20. In the present paper, the baseline geometry and grid for the present chemically reacting study are identical to that used in the inert mixing study,[7] where the grid-induced error with respect to the mixing parameters on a 3.6 million node mesh was verified not to exceed 10%. An upcoming paragraph will verify that the additional chemical processes present in the current study are accurately modeled with the same grid density.

Ignition Location and Flame Development

The governing equations with Jachimowski chemical kinetics are solved on a 3.6 million node mesh fitting the geometry detailed in Figs. 2 and 3, herein referred to as the baseline inlet. Figures 4 and 5 show the flame location and development in the baseline inlet. Figure 4 shows both pressure and H_2O mass fractions on the plane that cuts through the center of an injector ($z = 0$ m) and extends along the dual spike inlet (Fig. 3). The intersection of the two major inlet shocks indicates the position for the engine cowl and the relative size of the flame. Figure 5 shows both H_2 and H_2O contours on

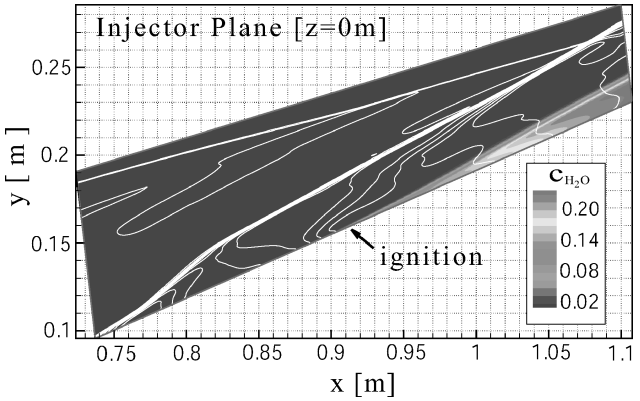

Fig. 4 Location of premature ignition in the baseline inlet, contour lines represent pressure, contour flood represents c_{H_2O}.

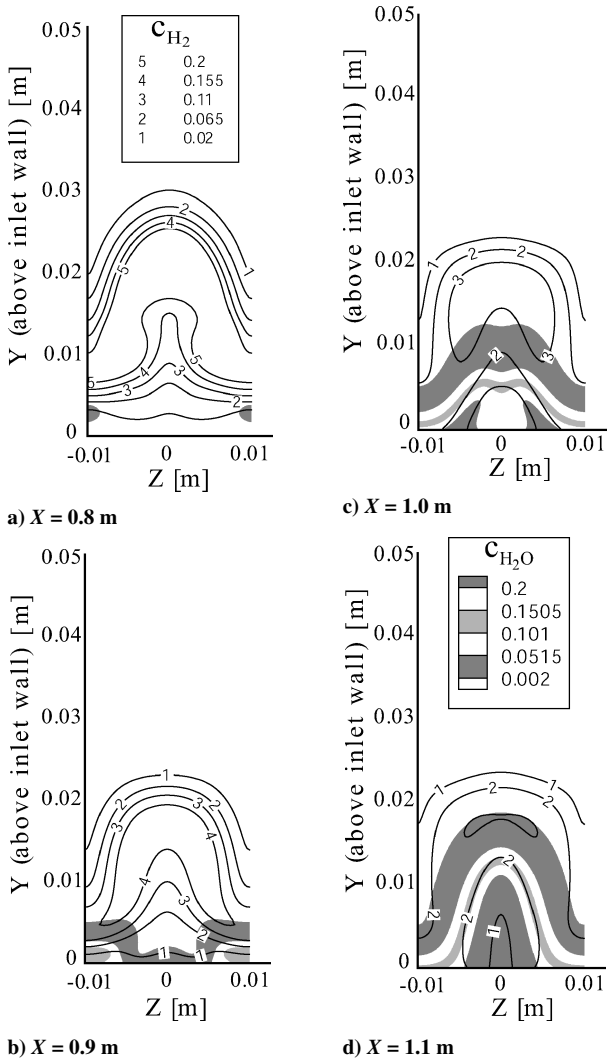

Fig. 5 Flame development in the baseline inlet, contour lines represent c_{H_2}, contour flood represents c_{H_2O}.

various yz planes starting from the point of first ignition. Ignition is seen to occur at $z = \pm 1$ cm (between injectors) when a near-stoichiometric hydrogen/air mixture ($c^S_{H_2} = 0.02876$) first enters the boundary layer. The initial reactive species are then swept toward the $z = 0$ cm plane by axial vortices, and the flame quickly spreads into the core flow. Note that by $x = 1.1$ m the flame has spread throughout most of the hydrogen/air mixture. Analysis of the flowfield reveals that the second compression process (in this case the second inlet shock) is the dominant mechanism that causes the fuel/air mixture to enter the boundary layer. The air buffer created by the cantilevered injector is significantly compressed through this shock, and because the fuel/air mixture has spread to the symmetry boundary, the axial vortices transport a combustible mixture into the already diminished air buffer. This mechanism is shown in Fig. 6a, which also shows the resulting hot spot in the boundary layer between injectors that is not influenced by the axial vortices. The diffusion of combustible mixture into this high-temperature region is what triggers ignition in the baseline inlet.

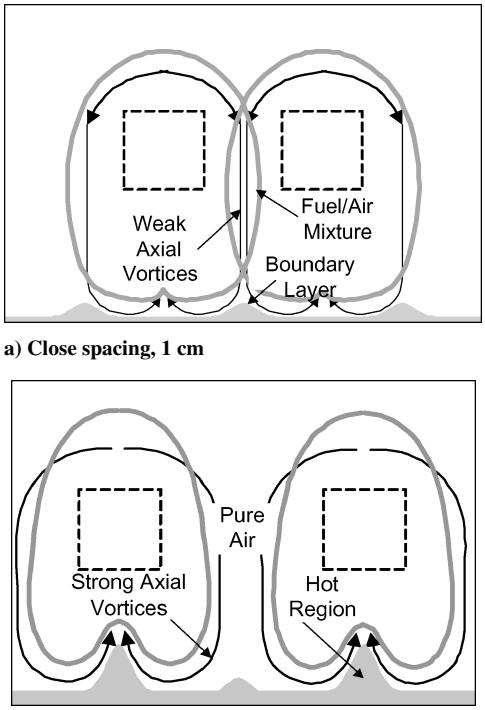

Fig. 6 Mechanism by which axial vortices affect the air buffer generated by the cantilevered ramp injector.

The previous inert mixing study[7] suggests two inlet modifications to lower the risk of premature ignition. The first modification involves using the Prandtl–Meyer compression fan used in the inert mixing study (see Ref. 7) instead of the second inlet spike. The resulting chemically reacting flowfield is shown in Fig. 7. Here, the compression process is not as sudden as with a shock. As a result, the air buffer erodes more slowly and ignition in the boundary layer is slightly delayed. The mixture still ignites, however, and the axial vortices spread the flame into the core flow before the inlet exit. The second modification simply increases the spacing between injectors from 1 to 2 cm. This allows the axial vortices to transport pure air into the buffer area and, hence, delays the presence of a combustible mixture in the boundary layer. In addition, the hot spot between injectors is now farther away from the combustible mixture due to the higher injector spacing. However, as shown in Fig. 6b, the unobstructed (and thus stronger) axial vortices entrain hot air from the boundary layer into the mixing layer. The flowfield resulting from this modified inlet was solved with Jachimowski chemical kinetics on a 7 million node mesh (to maintain the same grid density). As can be seen in Fig. 8, ignition in the boundary layer is only delayed, and in addition, the core flow ignites before the inlet exit. Thus, in all three configurations, premature ignition is found to occur only in the last 15% of the total inlet length. However, at the inlet exit the flame has already spread through a significant amount of the fuel/air mixture. Combustion in the inlet is detrimental to the efficiency of the shcramjet engine and must be suppressed. The remainder of this paper will focus on suppressing premature ignition in the boundary layer of the baseline inlet.

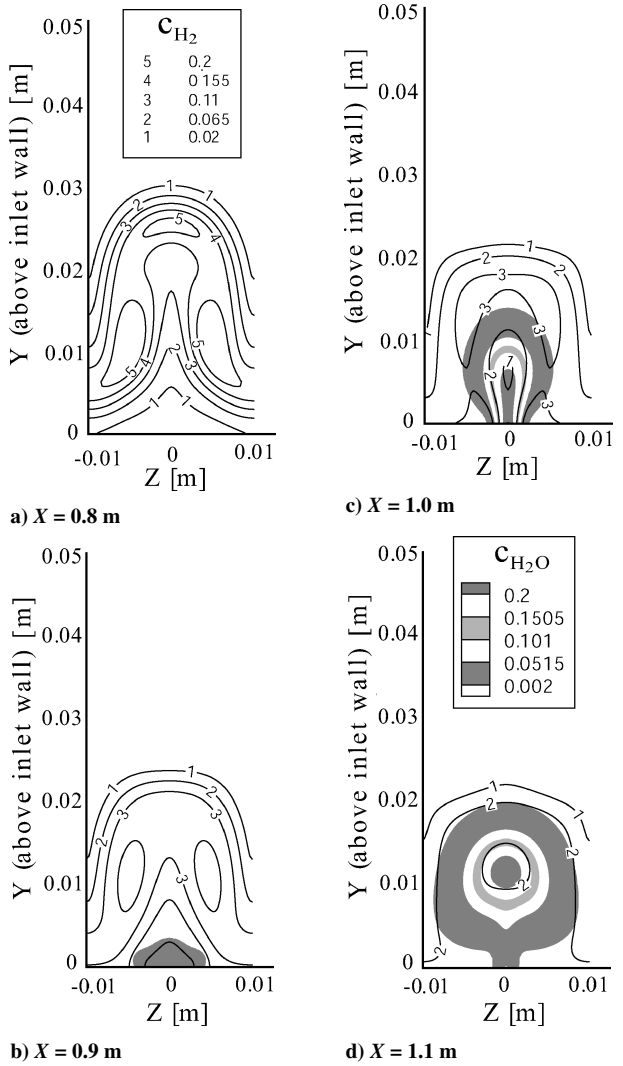

Fig. 7 Flame development in the compression fan inlet, contour lines represent c_{H_2}, contour flood represents c_{H_2O}.

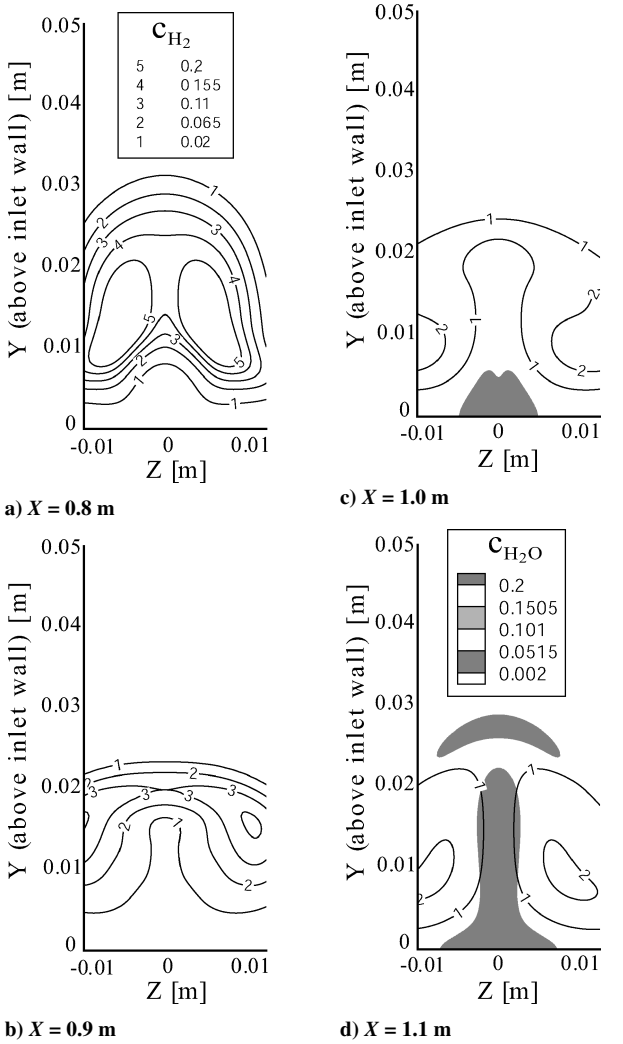

Fig. 8 Flame development in the wide-spaced injection inlet, contour lines represent c_{H_2}, contour flood represents c_{H_2O}.

Inlet Performance Parameters

Although nitrogen or additional hydrogen injection may be necessary to suppress premature ignition in a shcramjet inlet, it must not reduce the mixing efficiency or increase the inlet losses substantially. The air-based mixing efficiency η_m at the station of interest (here denoted by the subscript b) is defined as the ratio between the mass flux of oxygen that would react and the mass flux of oxygen entering the engine:

$$\eta_m \equiv \int_b c^R_{O_2} \frac{d\dot{m}}{0.235 \dot{m}_{air,engine}} \tag{1}$$

Here, the mass fraction of reacting oxygen, $c^R_{O_2}$, corresponds to

$$c^R_{O_2} = \min\left(c_{O_2}, c^S_{O_2} c_{H_2} / c^S_{H_2}\right) \tag{2}$$

with the stoichiometric mass fraction of hydrogen $c^S_{H_2}$ equal to 0.02876 and the stoichiometric mass fraction of oxygen $c^S_{O_2}$ equal to 0.22824. Inlet losses are captured by the normalized frictional force in the x direction, $\mathcal{F}^x_{\text{skin friction}}$, which corresponds to the skin-friction force experienced by the inlet in the x direction, normalized by the mass flow rate of air entering the engine, $\dot{m}_{air,engine}$.

Grid Convergence

A detailed grid convergence study with respect to the mixing parameters on the 3.6 million node baseline mesh found a grid induced error of 10% (Refs. 7 and 10). In three-dimensional numerical simulations, it is difficult to refine the mesh sufficiently to assess the grid-induced error accurately. Only the variation of results between different mesh densities is available. The grid-induced error was, thus, approximated by comparing the variation in mixing efficiency between specific mesh densities in three dimensions to the corresponding variations observed in the same mesh densities in two dimensions. The mixing efficiency was found to vary by 3% from fine to coarse meshes in three dimensions, which resulted in an approximated grid-induced error of 10% (Refs. 7 and 10). In the present study, the baseline configuration including chemical kinetics is solved on similar mesh densities of 1.1, 2.0, 3.6, and 6.5 million nodes. To approximate the magnitude of the grid-induced error with respect to the combustion processes, the mixing efficiency (an integrated result) along with the maximum H_2O mass fraction on each yz plane are selected and verified for convergence. Figures 9 and 10 show the results in the region of premature combustion. Figure 9 reveals variations in mixing efficiency (averaged in the combustion region) of 4.3, 2.4, and 1.0% for the 1.1, 2.0, and 3.6 million node meshes respectively, when compared with the 6.5 million node mesh. The variation of 4.3% in mixing efficiency from fine to coarse meshes is only slightly higher than 3% for the inert mixing study, and so a similar grid-induced error of 10% is inferred for the present chemically reacting study. In addition, continued use of the 3.6 million node mesh is also justified because the average variation compared to the 6.5 million node mesh is only 1.0%. Figure 10 shows how all four mesh densities predict the same ignition location and also display convergence of the flame propagation. The ignition

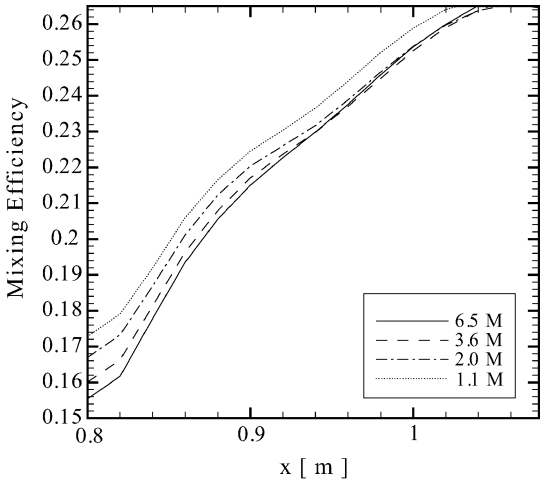

Fig. 9 Grid convergence of mixing efficiency in combustion region.

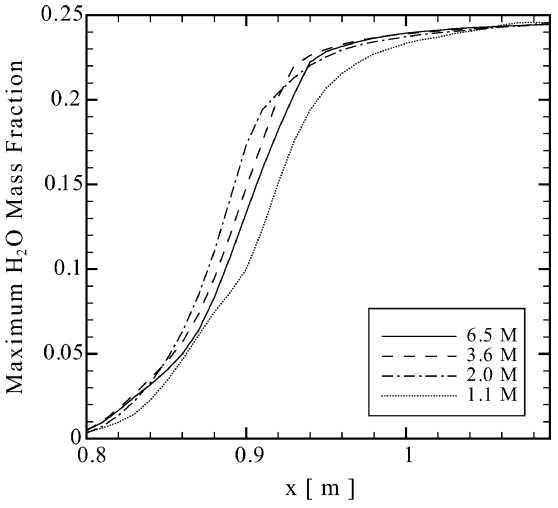

Fig. 10 Grid convergence of ignition location and flame propagation.

location is an important result and is seen to be modeled with sufficient accuracy by the 3.6 million node mesh.

Nonreacting Flowfield Analysis

The high mesh densities used for this study and the inclusion of Jachimowski chemical kinetics are very demanding in terms of computational time and memory. It is practical, therefore, to first analyze the inert flowfield (without chemistry) and choose only the most promising strategies for a full chemically reacting study. The first set of modified inlets attempt to cool the boundary layer with injection of an inert gas (nitrogen). Three selected strategies are presented. The first is called the N_2 Window and is detailed in Fig. 11. Here, nitrogen is injected between the hydrogen fuel and the boundary layer without requiring any new protrusions in the flow. The remainder of the inlet remains unchanged from the baseline inlet. The second and third strategies, detailed in Figs. 12 and 13, are called postshock and preshock injection, respectively. Here, nitrogen is injected through a slot 5 mm in height (slightly higher than the incoming boundary layer) both after ($x = 0.75$ m) and before ($x = 0.69$ m) the second inlet spike of the inlet. In both cases, the pressure of injected nitrogen matches the surrounding flow pressure and the velocity is approximately half that of the surrounding flow.

The resulting nonreacting flow fields are shown near the ignition location, $x = 0.85$, for each strategy and compared with the baseline inlet in Fig. 14. Here, results are indicated by contours of temperature

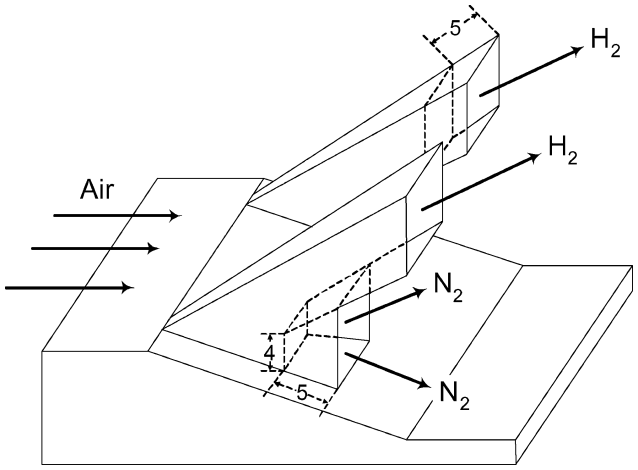

Fig. 11 N_2 Window injection, q_{N_2} = 750 m/s, p_{N_2} = 10 kPa, and T_{N_2} = 100 K, with dimensions in millimeters; see Fig. 2 for missing dimensions.

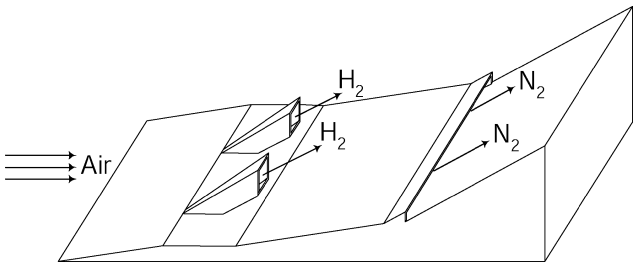

Fig. 12 Postshock slot injection, q_{N_2} = 1500 m/s, p_{N_2} = 15 kPa, and T_{N_2} = 100 K.

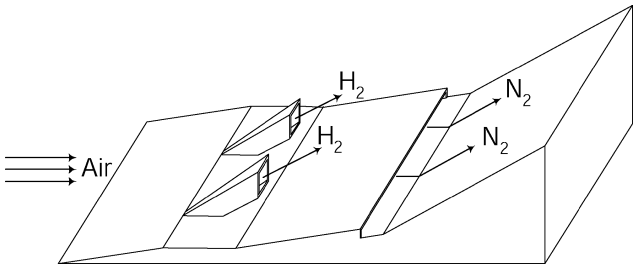

Fig. 13 Preshock slot injection, q_{N_2} = 1500 m/s, p_{N_2} = 6 kPa, and T_{N_2} = 100 K.

overlayed by a shaded region representing the hydrogen/air mixture. It can be seen that, without any attempt to cool the boundary layer, the initial region where fuel/air mixture enters the boundary layer in the baseline inlet is consistent with the actual ignition location determined with chemical kinetics, shown earlier in Fig. 5. The N_2 Window configuration not only fails to cool the boundary layer but is seen to actually entrain hot air from the boundary layer into the core flow. In contrast, both the postshock and preshock slot injection succeed in cooling the boundary layer significantly. As seen in Fig. 14, temperatures over 1000 K have been reduced to two small regions. By the injection of the nitrogen before the shock, it has a longer distance to mix and cool the boundary layer, and hence, the preshock injection is seen to be more effective. More important, because the injection pressure is matched to the surrounding flow, the preshock strategy injects nitrogen at a much lower pressure, which corresponds to approximately 60% less nitrogen (by mass) than the postshock strategy. Each strategy is verified to have a negligible effect on both the mixing efficiency and skin-friction losses.

Chemically Reacting Flowfield Analysis

The chemically reacting flowfield resulting from the preshock nitrogen injection was then computed by including the Jachimowski

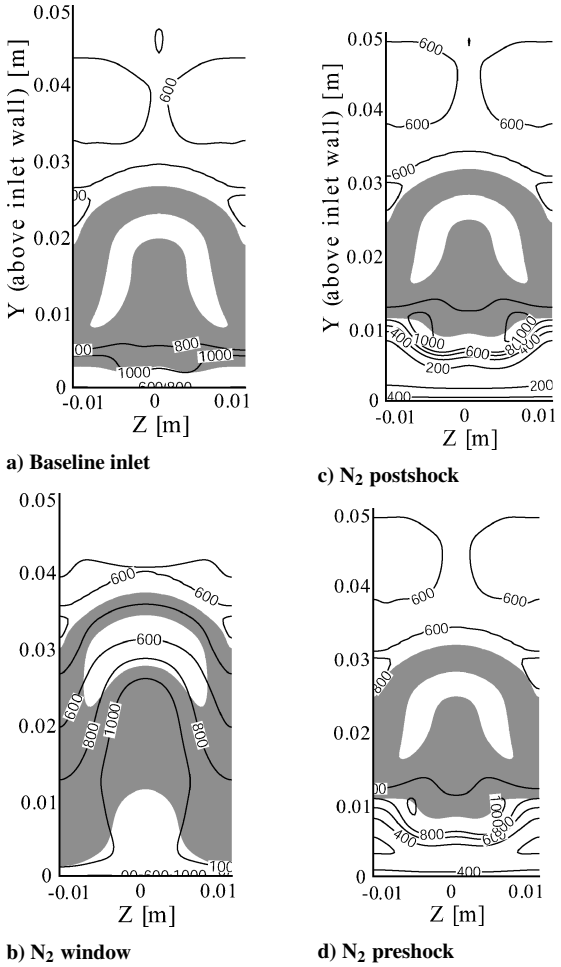

Fig. 14 Nitrogen injection strategies, shaded region represents hydrogen/air mixture, (0.8 < ϕ < 7.0) and contour lines represent temperature in Kelvin, X = 0.85 m.

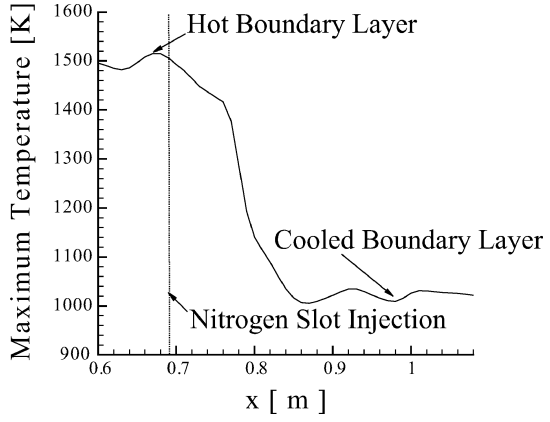

Fig. 15 Flame suppression via preshock nitrogen injection; successful boundary-layer cooling.

combustion model. Premature ignition is indeed prevented inasmuch as virtually no H_2O is present at the inlet exit. Figure 15 details the effect of nitrogen injection on the maximum temperature at each x plane. Although successful, the technical implementation of this strategy requires a source of cryogenic nitrogen, which is clearly impractical.

However, based on the results of the nitrogen slot injection, it is evident that injecting hydrogen through the slot may also suppress the flame. Indeed, the cantilevered injector succeeds in keeping the fuel/air mixture out of the boundary layer until the last 15% of the total inlet length. In addition, the nitrogen suppressed ignition solely because it cooled the boundary layer below ignition temperature before the fuel/air mixture arrived (as opposed to diluting the mixture such that it would not ignite). Thus, even though injecting hydrogen will create a new region of combustible flow, as long as the temperature is below that required for ignition, premature ignition will not occur.

Three strategies of injecting hydrogen are selected to portray both the successful suppression of premature ignition, as well as the minimization of additional hydrogen injected such that the global equivalence ratio does not exceed one. The strategies are denoted as H_{2slot1}, H_{2slot2}, and H_{2slot3}. The gas properties at injection for each case are summarized in Table 1. The resultant three chemically reacting flowfields at the inlet exit, $x = 1.07$ m are shown in Fig. 16 along with the successful N_{2slot} preshock injection strategy for comparison. Initially, hydrogen is injected in the preshock configuration seen in Fig. 13 at the same temperature and pressure as the N_{2slot} case, however, at velocity of 5257 m/s matching that out of the cantilevered injectors (case H_{2base}). As seen in Fig. 16, the high injection velocity of H_{2slot1} results in better mixing and lower temperatures at the inlet exit compared with the N_{2slot} case. However, this low-temperature hydrogen is not ignited via the shock-induced combustion process and so does not contribute to the heat release in the combustor. For this reason, the H_{2slot2} strategy injects the hydrogen at a higher temperature. Specifically the hydrogen is injected at the same conditions as for the cantilevered injectors with the exception that the pressure is maintained at 6 kPa to match the surrounding flow. Figure 16 confirms that this strategy also succeeds in keeping the mixture below ignition temperatures but still close enough that the shock-induced combustion process will ignite the new mixture. Thus, the problem of suppressing premature ignition is reduced to adding an additional slot fuel injector. However, as Table 1 shows, injecting hydrogen in this manner results in a global equivalence ratio of 1.3. To reduce the global equivalence ratio to one, both the velocity and/or slot height must be reduced. It was determined that if the slot height is maintained at 5 mm, the required low injection velocity results in a detachment of the shock from the 12-deg inlet spike. The third strategy, H_{2slot3}, reduces the velocity as well as the slot height to 4 mm. The inflow conditions are again listed in Table 1, which result in $\phi_g = 1$. As seen in Fig. 16, the significantly lower mass flow of hydrogen has less capacity to absorb heat from the developing boundary layer than the earlier cases. As a result, temperatures over 1000 K are just beginning to develop at the inlet exit. Note, however, that, although this region appears as flammable mixture in Fig. 16 ($0.8 < \phi < 7$), it is still fuel rich ($\phi > 2.8$) and requires a temperature greater than 1000 K to initiate combustion. Premature ignition is considered suppressed for this case because the maximum mass fraction of H_2O does not exceed 2 ppm anywhere in the inlet. This leaves configuration H_{2slot3} as the most feasible configuration for a fully functioning shcramjet inlet.

Another potential method of reducing the mass flow of additional hydrogen is to use an array of expansion ramp injectors, shown in Fig. 17, instead of a continuous slot injector. In this configuration, not only is a new flammable region created above the injectors (as with the continuous slot injector), but also on the sides of the ramp injectors. This flammable region is now in direct contact with the boundary layer attached to the inlet wall. To determine if premature ignition occurs, the continuous slot injection grid was modified to inject hydrogen through 8.8-mm-wide, 5-mm-high expansion ramp injectors at the same location in the inlet, $x = 0.69$ m, centered on the same plane as the cantilevered injectors, $z = 0$ m. Table 1 shows the hydrogen properties at injection for this case, H_{2ramp}, whereas Fig. 18 shows the temperature and equivalence ratio fields at $x = 0.85$ m and $x = 0.90$ m. Analysis of the resulting chemically reacting flowfield determines premature ignition to occur at $x = 0.8$ m on the sides of the injector, where the newly created flammable mixture is exposed to ignition temperatures as shown in Fig. 18. Thus, continuous slot injection may be necessary for the sole purpose of keeping a fuel-rich region in contact with the inlet wall and the new fuel/air mixing region away from the wall. Note, however, that, if nitrogen is used

Table 1 Tabulated injection properties for the shcramjet inlet cases

Case	q, m/s	T, K	p, Pa	M_c	ϕ_g	T_{stag}, K	P_{stag}, kPa	$\mathcal{F}^x_{\text{skin friction}}$, N · s/kg
$H_{2\,\text{base}}$	5257	243	9600	1.2	0.82	1216	2448.0	42.1
$N_{2\,\text{slot}}$	1509	100	6000	−2.0	0.82	1200	35400.0	40.0
$H_{2\,\text{slot1}}$	5257	100	6000	1.6	1.40	1052	22670.0	39.3
$H_{2\,\text{slot2}}$	5257	243	6000	1.2	1.30	1216	1571.0	36.8
$H_{2\,\text{slot3}}$	2500	243	6000	−0.3	1.00	437	47.0	37.7
$H_{2\,\text{ramp}}$	5257	243	4000	1.2	0.96	1216	1047.0	38.7

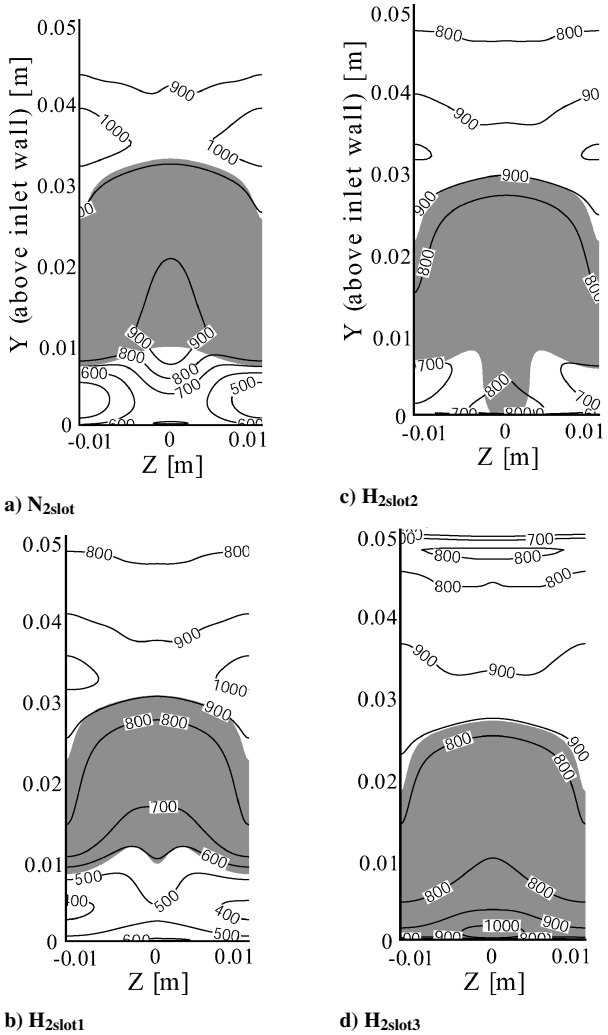

Fig. 16 Suppression of premature ignition at inlet exit, shaded region represents hydrogen/air mixture ($0.8 < \varphi < 7.0$), and contour lines represent temperature in Kelvin, $X = 1.07$ m.

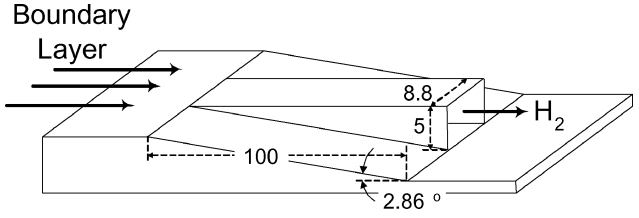

Fig. 17 Expansion ramp injector, dimensions in millimeters.

as the coolant gas, the initial mixture in contact with the hot inlet wall will no longer be flammable. Thus, the expansion ramp injector configuration may still be a feasible way of reducing the mass flow of nitrogen necessary to prevent premature ignition.

In addition to preventing premature ignition in the shcramjet inlet, the injection of cool gas along the inlet wall has the potential to reduce the frictional force felt by the shcramjet wall. Table 1 shows the variation in $\mathcal{F}^x_{\text{skin friction}}$ for the various configurations. As expected, nitrogen injection creates the same amount of friction as the air boundary layer in the baseline case. The highest mass flux of hydrogen injected, case $H_{2\text{slot1}}$, is found not to reduce the skin friction. However, as the mass flux is reduced, a reduction in skin friction of roughly 10% is observed. The added surface area in the expansion ramp configuration is seen to add slightly to the frictional force.

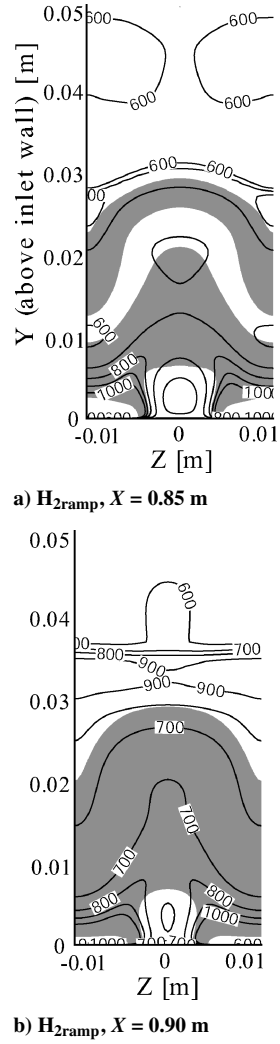

Fig. 18 Expansion ramp injector flowfield, shaded region represents hydrogen/air mixture ($0.8 < \varphi < 7.0$), and contour lines represent temperature in Kelvin.

Conclusions

Premature ignition was found to occur in all three previously recommended optimal shcramjet inlets. The cantilevered ramp injectors do succeed in keeping the fuel/air mixture out of the boundary layer until the last 15% of the inlet. However, at this point the second inlet shock compresses the mixture into the boundary layer, where it ignites and quickly spreads into the core flow before the inlet exit. Slot injection of additional coolant gas just before the second inlet spike was determined to be the optimal configuration through analysis of various nonreacting strategically modified inlets. Chemically

reacting simulations then verified that injection of both nitrogen and hydrogen through the slot suppress premature ignition while maintaining the performance of the original inlet.

Finally, numerical simulation yields a feasible configuration for a fully functional shcramjet inlet. Hydrogen fuel is injected through an infinite array of cantilevered ramp injectors at a convective Mach number of 1.2 and global equivalence ratio of 0.82. Mixing is enhanced by turbulence, the stretching of the fuel/air interface due to strong axial vortices, and the compression processes in the inlet. Additional hydrogen is injected through a continuous, 4-mm-high slot injector just before the second inlet spike, such that the global equivalence ratio is raised to one. The hydrogen, although injected at 243 K, is enough to cool the incoming boundary layer before the fuel/air mixture is compressed into this region by the second inlet shock. As a result, the flammable mixture does not ignite at any point in the shcramjet inlet. The resulting mixture is at an average temperature of 900 K, a global equivalence ratio of one, and mixed at 30% efficiency at the exit of the inlet. In addition, the frictional force experienced by the inlet is reduced by 10% due to the injected hydrogen along the inlet wall.

Acknowledgment

This work has been supported by the Natural Sciences and Engineering Research Council. The third author acknowledges the support of the BK21 program.

References

[1]Sislian, J. P., and Atamanchuk, T. M., "Aerodynamic and Propulsive Performance of Hypersonic Detonation Wave Ramjets," *Proceedings of the 9th International Symposium on Airbreathing Engines*, AIAA, Washington, DC, 1989, pp. 1026–1035.

[2]Dudebout, R., Sislian, J. P., and Oppitz, R., "Numerical Simulation of Hypersonic Shock-Induced Combustion Ramjets," *Journal of Propulsion and Power*, Vol. 14, No. 6, 1998, pp. 869–879.

[3]Seiner, J. M., Dash, S. M., and Kenzakowski, D. C., "Historical Survey on Enhanced Mixing in Scramjet Engines," *Journal of Propulsion and Power*, Vol. 17, No. 6, 2001, pp. 1273–1286.

[4]Livingston, T., Segal, C., Schindler, M., and Vinogradov, V. A., "Penetration and Spreading of Liquid Jets in an External–Internal Compression Inlet," *AIAA Journal*, Vol. 38, No. 6, 2000, pp. 989–994.

[5]Owens, M., Mullagiri, S., Segal, C., and Vinogradov, V. A., "Effects of Fuel Preinjection on Mixing in Mach 1.6 Airflow," *Journal of Propulsion and Power*, Vol. 17, No. 3, 2001, pp. 605–610.

[6]Guoskov, O. V., Kopchenov, V. I., Lomkov, K. E., and Vinogradov, V. A., "Numerical Research of Gaseous Fuel Preinjection in Hypersonic Three-Dimensional Inlet," *Journal of Propulsion and Power*, Vol. 17, No. 6, 2001, pp. 1162–1169.

[7]Sislian, J. P., and Parent, B., "Hypervelocity Fuel/Air Mixing in a Shcramjet Inlet," *Journal of Propulsion and Power*, Vol. 20, No. 2, 2004, pp. 263–272.

[8]Sislian, J. P., and Schumacher, J., "A Comparative Study of Hypersonic Fuel/Air Mixing Enhancement by Ramp and Cantilevered Ramp Injectors," AIAA Paper 99-4873, Nov. 1999.

[9]Marble, F., Zukoski, E., Jacobs, J., Hendricks, G., and Waitz, I., "Shock Enhancement and Control of Hypersonic Mixing and Combustion," AIAA Paper 90-1981, July 1990.

[10]Parent, B., Sislian, J. P., and Schumacher, J., "Numerical Investigation of the Turbulent Mixing Performance of a Cantilevered Ramp Injector," *AIAA Journal*, Vol. 40, No. 8, 2002, pp. 1559–1566.

[11]Parent, B., and Sislian, J. P., "Effect of Geometrical Parameters on the Mixing Performance of Cantilevered Ramp Injectors," *AIAA Journal*, Vol. 41, No. 3, 2003, pp. 448–456.

[12]Parent, B., and Sislian, J. P., "The Use of Domain Decomposition in Accelerating the Convergence of Quasihyperbolic Systems," *Journal of Computational Physics*, Vol. 179, No. 1, 2002, pp. 140–169.

[13]Wilcox, D. C., "Reassessment of the Scale Determining Equation for Advanced Turbulence Models," *AIAA Journal*, Vol. 26, No. 11, 1988, pp. 1299–1310.

[14]Yee, H. C., Klopfer, G. H., and Montagné, J.-L., "High-Resolution Shock-Capturing Schemes for Inviscid and Viscous Hypersonic Flows," *Journal of Computational Physics*, Vol. 88, No. 1, 1990, pp. 31–61.

[15]Wilcox, D. C., "Dilatation–Dissipation Corrections for Advanced Turbulence Models," *AIAA Journal*, Vol. 30, No. 11, 1992, pp. 2639–2646.

[16]Jachimowski, C. J., "An Analytical Study of the Hydrogen–Air Reaction Mechanism with Application to Scramjet Combustion," NASA TP 2791, Dec. 1988.

[17]McBride, B. J., and Reno, M. A., "Coefficients for Calculating Thermodynamic and Transport Properties of Individual Species," NASA TM 4513, Oct. 1993.

[18]Wilcox, D. C., *Turbulence Modeling for CFD*, DCW Industries, La Cañada, CA, 1994.

[19]Parent, B., and Sislian, J. P., "Validation of the Wilcox k-Omega Model for Flows Characteristic to Hypersonic Airbreathing Propulsion," *AIAA Journal*, Vol. 42, No. 2, 2004, pp. 261–270.

[20]Fusina, G., "Numerical Investigation of Oblique Detonation Waves for a Shcramjet Combustor," Ph.D. Dissertation, Graduate Dept. of Aerospace Science and Engineering, Univ. of Toronto, Toronto, ON, Canada, Aug. 2003.